NASA/TM—2006-214049

Smectic A Filled Birefringent Elements and Fast Switching Twisted Dual Frequency Nematic Cells Used for Digital Light Deflection

Oleg Pishnyak, Andrii Golovin, and Liubov Kreminska
Kent State University, Liquid Crystal Institute, Kent, Ohio

John J. Pouch and Félix A. Miranda
Glenn Research Center, Cleveland, Ohio

Bruce K. Winker
Rockwell Scientific Company LLC, Thousand Oaks, California

Oleg D. Lavrentovich
Kent State University, Liquid Crystal Institute, Kent, Ohio

September 2006

NASA STI Program . . . in Profile

Since its founding, NASA has been dedicated to the advancement of aeronautics and space science. The NASA Scientific and Technical Information (STI) program plays a key part in helping NASA maintain this important role.

The NASA STI Program operates under the auspices of the Agency Chief Information Officer. It collects, organizes, provides for archiving, and disseminates NASA's STI. The NASA STI program provides access to the NASA Aeronautics and Space Database and its public interface, the NASA Technical Reports Server, thus providing one of the largest collections of aeronautical and space science STI in the world. Results are published in both non-NASA channels and by NASA in the NASA STI Report Series, which includes the following report types:

- TECHNICAL PUBLICATION. Reports of completed research or a major significant phase of research that present the results of NASA programs and include extensive data or theoretical analysis. Includes compilations of significant scientific and technical data and information deemed to be of continuing reference value. NASA counterpart of peer-reviewed formal professional papers but has less stringent limitations on manuscript length and extent of graphic presentations.

- TECHNICAL MEMORANDUM. Scientific and technical findings that are preliminary or of specialized interest, e.g., quick release reports, working papers, and bibliographies that contain minimal annotation. Does not contain extensive analysis.

- CONTRACTOR REPORT. Scientific and technical findings by NASA-sponsored contractors and grantees.

- CONFERENCE PUBLICATION. Collected papers from scientific and technical conferences, symposia, seminars, or other meetings sponsored or cosponsored by NASA.

- SPECIAL PUBLICATION. Scientific, technical, or historical information from NASA programs, projects, and missions, often concerned with subjects having substantial public interest.

- TECHNICAL TRANSLATION. English-language translations of foreign scientific and technical material pertinent to NASA's mission.

Specialized services also include creating custom thesauri, building customized databases, organizing and publishing research results.

For more information about the NASA STI program, see the following:

- Access the NASA STI program home page at *http://www.sti.nasa.gov*

- E-mail your question via the Internet to *help@sti.nasa.gov*

- Fax your question to the NASA STI Help Desk at 301–621–0134

- Telephone the NASA STI Help Desk at 301–621–0390

- Write to:
  NASA STI Help Desk
  NASA Center for AeroSpace Information
  7121 Standard Drive
  Hanover, MD 21076–1320

NASA/TM—2006-214049

Smectic A Filled Birefringent Elements and Fast Switching Twisted Dual Frequency Nematic Cells Used for Digital Light Deflection

Oleg Pishnyak, Andrii Golovin, and Liubov Kreminska
Kent State University, Liquid Crystal Institute, Kent, Ohio

John J. Pouch and Félix A. Miranda
Glenn Research Center, Cleveland, Ohio

Bruce K. Winker
Rockwell Scientific Company LLC, Thousand Oaks, California

Oleg D. Lavrentovich
Kent State University, Liquid Crystal Institute, Kent, Ohio

National Aeronautics and
Space Administration

Glenn Research Center
Cleveland, Ohio 44135

September 2006

Acknowledgments

We thank Phil Bos and Sergij Shiyanovskii for numerous useful discussions. The work was supported by NASA grant NAG3–2539 and by Rockwell Scientific Company.

Level of Review: This material has been technically reviewed by technical management.

Available from

NASA Center for Aerospace Information
7121 Standard Drive
Hanover, MD 21076–1320

National Technical Information Service
5285 Port Royal Road
Springfield, VA 22161

Available electronically at http://gltrs.grc.nasa.gov

Smectic A Filled Birefringent Elements and Fast Switching Twisted Dual Frequency Nematic Cells Used for Digital Light Deflection

Oleg Pishnyak, Andrii Golovin, and Liubov Kreminska
Kent State University
Liquid Crystal Institute
Kent, Ohio 44242

John J. Pouch and Félix A. Miranda
National Aeronautics and Space Administration
Glenn Research Center
Cleveland, Ohio 44135

Bruce K. Winker
Rockwell Scientific Company LLC
Thousand Oaks, California 91360

Oleg D. Lavrentovich
Kent State University
Liquid Crystal Institute
Kent, Ohio 44242

Abstract

We describe the application of smectic A (SmA) liquid crystals for beam deflection. SmA materials can be used in digital beam deflectors (DBDs) as fillers for passive birefringent prisms. SmA prisms have high birefringence and can be constructed in a variety of shapes, including single prisms and prismatic blazed gratings of different angles and profiles. We address the challenges of uniform alignment of SmA, such as elimination of focal conic domains. Fast rotation of the incident light polarization in DBDs is achieved by an electrically switched 90° twisted nematic (TN) cell.

1. Introduction

Beam steering devices are in a great demand in free space laser communications, optical fiber communications, optical switches, scanners (refs. 1 to 5), etc. In addition to mechanical devices such as gimbals and mirrors, a number of other techniques are under development, such as ceramic-based phase gratings (ref. 2), micro-electromechanical relief gratings (ref. 3), micromirror devices (ref. 4), decentered lens arrays, thermo-optic deflectors (ref. 5), photonic crystals (ref. 6), etc. Liquid crystals (LCs) are of special interest as active materials in non-mechanical beam steerers and deflectors, because they promise low size, weight, operating voltage, and low-cost fabrication (refs. 1 and 7). Recent advances in the synthesis of new LC materials (ref. 8) and in the design of the nematic LC cells (ref. 9) significantly improved parameters important for effective beam steering, such as optical birefringence and response time.

One of the most promising areas for LC-based systems is NASA's near-Earth and deep-space missions that require precise, diffraction-limited (sub-microradian), electronic (non-mechanical) beam steering as well as in situ wave-front correction. LC-based systems are inexpensive, light-weight and low-power. LC optical phased arrays could be used as part of a tracking network that supports high-data-rate communication links between the planetary rovers, the host lander, the orbiting spacecraft, and space

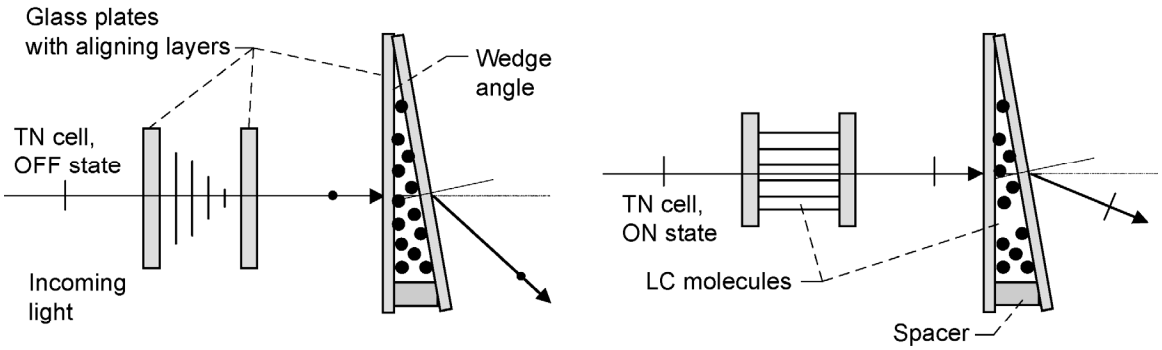

Figure 1.—The principal scheme of a beam deflecting stage, composed of the switchable polarization rotator (90° TN cell) and a passive prism made of a SmA wedge. Both elements can be replaced: for example, a crystalline prism can be used as a deflector or an electrically-controlled birefringence cell can be used as a polarization rotator.

platforms; autonomous operation of the rovers and robotic systems; and possibly strategic mining operations.

The most popular liquid crystal-based beam steering devices are based on diffractive and prismatic designs. Diffractive LC devices are known at least since 1974, when Borel et al. described a binary rectangular LC diffraction grating (ref. 10). This approach has been expanded by optical-array beam steerers (refs. 1, 11 to 14), polymer-dispersed liquid crystal gratings (ref. 15), ferroelectric liquid crystal gratings (ref. 16), photonic crystals filled with liquid crystals (ref. 6) and voltage-controlled cholesteric liquid crystal gratings capable of both Raman-Nath and Bragg diffraction (refs. 17 and 18).

Among the prism-based DBDs, one of the most effective designs uses a cascade of elementary stages each of which represents a pair consisting of an active polarization rotator and a prismatic deflector (refs. 19 to 26). The advantage of such a decoupled design is that it allows one to separate the issue of the short response time (determined mostly by the switching speed of the rotator) and the angular range of deflection (determined by the geometry and optical properties of the deflector). For example, the active element can be electrically switched by a 90° TN cell followed by a passive birefringent prism that separates the beam into two channels, depending on the beam polarization (fig. 1). Depending on the applied voltage, the TN cell rotates the polarization of incident light by $\pi/2$ (no field, OFF state) or leaves the polarization intact (when the applied electric field reorients the liquid crystal molecules perpendicular to the plates of the cell, ON state). Inside the prism, the beam propagates in ordinary or extraordinary mode, depending on the polarization. As the ordinary and extraordinary refractive indices are different, the two modes of propagation through the prism result in different angles of deflection. As is clear from figure 1, if the SmA prism is used, the optical axis (and thus the preferred orientation of the SmA molecules) should be aligned along the edge of the wedge. In this geometry the director field is uniform everywhere. The decoupled pair of a rotator and deflector has no moving parts and can be cascaded into N stages, making 2^N addressable beam directions (refs. 19 to 26). The liquid crystals can be used in both active and passive elements of prism-based DBDs, as they demonstrate a relatively high optical birefringence (in the range 0.1 to 0.4) and relatively fast switching speeds (milliseconds or less), (see, for example, ref. 9). Application of LCs for polarization switching is a well-developed field, mostly because the TN and similar nematic cells are at the heart of modern LC display devices (ref. 27).

Application of LCs in the passive prismatic elements is less studied, despite their apparent advantages, such as structural flexibility and low-cost fabrication. One of the reasons for such a neglect is that a LC-based prism with a substantial dihedral angle a (needed for the substantial angle of beam deflection) and a substantial aperture A should be relatively thick, up to $h = A \tan a$. If h is in the range of millimeters and centimeters, then huge losses caused by light scattering at director fluctuations (refs. 28 and 29) rule out the applicability of the nematic LCs. In this article we describe passive prismatic elements formed by a uniaxial SmA LC. The advantage of the SmA materials over nematic LCs is that director fluctuations are suppressed by the layered smectic structure.

The article is organized as follows. Section 2 discusses the alignment procedures of SmA. Section 3 presents optical properties of single prisms and arrays of polymer prisms filled with SmA. Section 4 describes the electro-optical properties of 90° TN cells filled with dual-frequency nematic. The conclusions are presented in section 5.

2. SmA LC Materials

In SmA, the elongated rod-like molecules are arranged in a periodic stack of layers with the director **n** (a unit vector that shows the average local direction of molecules and thus the optic axis of the material) being perpendicular to the layers; the states **n** and **–n** are identical. Inside the layer the molecular centers of gravity show no long-range order, thus each layer is a two-dimensional fluid. Positional order along **n** significantly reduces thermal director fluctuations and thus reduces light scattering (refs. 28 and 29). However, the very same layered structure brings about another possible source of scattering, namely, static director distortions such as undulations and focal conic domains (FCDs) (refs. 30 to 33). The problem is especially pronounced for the highly birefringent cyanobiphenyl materials in which the molecules form partially overlapped pairs with oppositely oriented dipole moments. The thickness of smectic layers in these materials is about 1.4 to 1.6 of the length of an individual molecule and can vary significantly with temperature; the changes in layer thickness result in director distortions. For example, cooling of the SmA material 4-octyloxy-4'-cyanobiphenyl (8OCB) in the planar cell with polyisoprene-coated substrates (ref. 34) results in layer undulations and formation of FCDs clearly visible in figure 2. These FCDs can be stabilized by a mechanical impurity in the bulk or at the surface of the cell (ref. 30). In principle, one can use a magnetic field to align the SmA sample uniformly (refs. 31 and 32). We quantify the process of field alignment of SmA by considering the behavior of an isolated FCD. The method might be effective if large magnetic fields are available. The model predicts that for each value of the applied field, there is a characteristic size of the FCD below which the domain cannot be transformed into the uniform state.

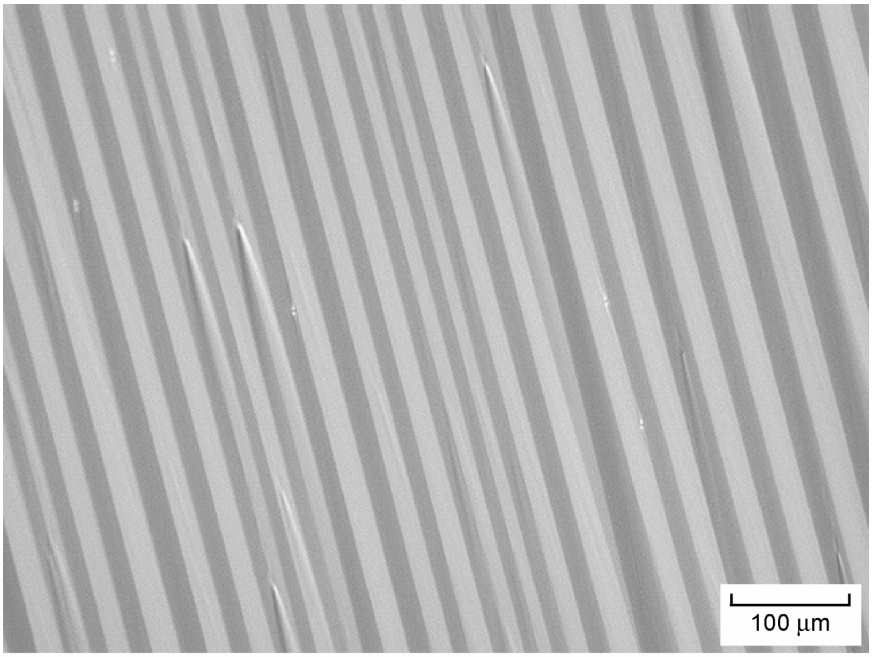

Figure 2.—Polarizing-microscope texture of an undulation pattern in SmA material 8OCB created by periodic director variations. The SmA was cooled down from the magnetically aligned nematic phase. Aligning layer: polyisoprene, no rubbing.[34] Cell thickness of 5 μm.

To obtain a close estimate of the magnetic field needed to align the SmA uniformly, we consider the simplest type of FCD, the so-called toric FCD that can be stabilized by a foreign particle in the SmA bulk (refs. 35 and 36). The toric FCD is based on a pair of linear defects, a circular defect line and the straight line passing through the center. The smectic layers are wrapped around the pair as shown in figure 3. Note that outside the FCD the molecules are oriented uniformly along a single axis parallel to the plates.

Suppose a small toric FCD with the radius a of the defect circle much smaller than the lateral size of the cell, is stabilized in an otherwise uniform SmA sample by a particle, which sets tangential orientation of SmA molecules at its surface. For the sake of simplicity, we approximate the particle by a disk of radius R (fig. 3). If the SmA were uniform, the director would be in an unfavorable perpendicular orientation at the plate. The FCD would be stable if its elastic energy (ref. 37)

$$F_{el} = 2\pi^2 aK\left[\ln\left(2a/r_c\right) - 2 - \overline{K}/K\right] + F_c , \tag{1}$$

(where K is the splay elastic constant, $\overline{K}$ is the saddle-splay constant, r_c is the core radius of the circular defect, and F_c is the core energy of the circle and the straight line) is smaller than the anchoring energy difference between the FCD-free (uniform) state and the FCD state:

$$\Delta F_s = 2\pi a^2 W , \tag{2}$$

where W is the (polar) surface anchoring coefficient at the SmA-particle interface. In SmA, $W \sim (10^{-3}–10^{-2})\text{J/m}^2$ is higher than the corresponding value in the nematic phase, $W \sim (10^{-5}–10^{-4})\text{J/m}^2$ (ref. 38).

If the anisotropy $\chi_a = \chi_{\parallel} - \chi_{\perp} > 0$ of SmA diamagnetic susceptibility is positive, then applying the field in the direction of the desired orientation of molecules should reduce the FCD, as the molecules inside the domain should reorient along **B** (fig. 3). The diamagnetic energy gain from such a reorientation is $\Delta F_B = 2\int \frac{1}{2}\mu_0^{-1}\chi_a B^2 \sin^2\theta dV$, where $\mu_0 = 4\pi\ 10^{-7}\text{N/A}^2$ is the permeability of free space, θ is the

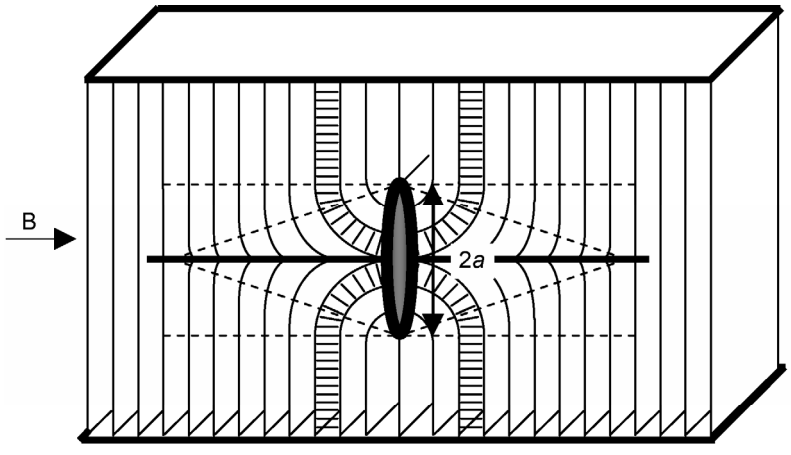

Figure 3.—Schematic view of toric FCD. The SmA layers are perpendicular to the substrates and folding within the FCD. The director changes the orientation on 90° from tangential outside the FCD to vertical within the FCD to satisfy the boundary conditions at the disk-like foreign particle in the SmA bulk.

angle between the director and **B**, the volume element is $dV = r(a - r\sin\theta)\sin\theta\, d\theta\, d\varphi\, dr$; r and $r - a/\sin\theta$ are the principal radii of curvature of SmA layers within the toric FCD, and r varies in the range from 0 to $a/\sin\theta$; $0 \le \theta \le \pi/2$; $0 \le \varphi < 2\pi$. Integration yields

$$\Delta F_B = \frac{1}{3}\pi \mu_0^{-1} \chi_a B^2 a^3 . \tag{3}$$

The stability of the FCD is determined by the energy difference between the FCD state and the uniform state, comprised of the elastic, surface anchoring, and diamagnetic contributions, $\Delta F = \Delta F_s - F_{el} - \Delta F_B$:

$$\Delta F = 2\pi a^2 W - 2\pi^2 a K \left[\ln\frac{2a}{r_c} - 2 - \frac{\bar{K}}{K} \right] - F_c - \frac{1}{3}\pi \mu_0^{-1} \chi_a B^2 a^3 . \tag{4}$$

Figure 4 shows the function $\Delta F(B)$ for four different sizes of FCDs, of radius a = 0.5, 1, 2, and 5 μm, calculated for the following typical values of parameters (refs. 29 and 38): $K = 10^{-11}$N, $\bar{K} = 0$, $W = 5*10^{-3}$J/m^2, r_c = 10 nm, $F_c = 0$ (r_c is chosen to adsorb the core energy into the elastic energy of layer distortions (ref. 28)), and $\chi_a = 10^{-5}$. The plot demonstrates that for each value of a, there is a critical value of the field for which ΔF becomes negative, i.e., the uniform state is energetically preferred over the FCD state.

The higher the field, the smaller is the size of the FCDs that can be transformed into the uniform state. However, to reduce the size of FCD to a practical sub-wavelength value, say, a = 0.5–1 μm, one needs huge magnetic fields of the order of tens and hundreds of Tesla (fig. 4). The alignment can be assisted by

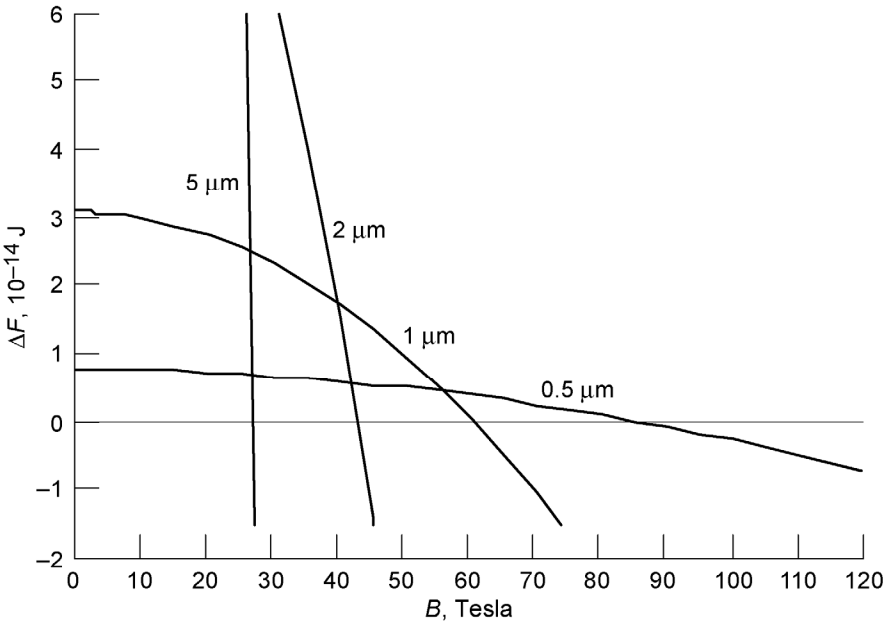

Figure 4.—Free energy difference between the uniform state of a SmA slab with an incorporated foreign particle-disk and the state with the toric FCD, as a function of the magnetic field applied to align the director uniformly. Different curves corresponding to the size of FCDs equal to 0.5, 1, 2, 5 μm.

applying the magnetic field while the material is in the nematic phase and then cooling it down to the SmA phase, as the surface anchoring in the nematic phase is much weaker that in the SmA phase.

The magnetic field needed to realign the director around the foreign inclusion in the nematic phase can de determined from the condition that the diamagnetic coherence length $\xi = \frac{1}{B}\sqrt{\frac{\mu_0 K}{\chi_a}}$ is smaller than the anchoring extrapolation length $l = \frac{K}{W}$:

$$B_c = W\sqrt{\frac{\mu_0}{KX_a}}\,. \tag{5}$$

For example, $B \sim 1$T would be sufficient to suppress the director distortions around a particle with $W \sim 10^{-5}$J/m^2; B ~ 10T would be needed if $W \sim 10^{-4}$J/m^2, etc. Therefore, magnetic alignment is easier in the nematic phase than in the SmA phase.

Consideration suggests that in order to minimize the light losses, one should search for the SmA material composed of nonpolar molecules in which the molecules do not form pairs and the layer thickness does not change much with temperature and in which there is a nematic phase, in addition to the SmA phase. The requirements are met by low-molecular weight materials belonging to the class of 4,4'-*n*-dialkylazoxybenzenes (refs. 22 and 23) (fig. 5(a)). We used n = 5,6,7, and 8 homologues of 4,4'-*n*-dialkylazoxybenzene purchased from Sigma-Aldrich Chemical Co. to prepare mixtures with a broad temperature range of the SmA phase. All components were purified to decrease the contents of undesired dopants and foreign particles. The purification process was as follows: first we dissolved the compound in methanol (99.93%, Aldrich) in proportion 1 g of LC in 100 ml of methanol. Then the solution was cooled down to separate the crystal from the methanol. The precipitated crystals were filtered and dried out. The purified compounds were mixed in various proportions to get the appropriate phase sequence and good alignment. The temperature range of SmA phase can be expanded to about 30° in eutectic mixtures. The mixture of n = 6 and n = 8 homologues in proportion 1:1 shows the best deflection efficiency (a ratio of intensities of the deflected and incident beams) and a good thermal range (fig. 5(b)). These mixtures were used as a SmA filler for passive prismatic deflectors.

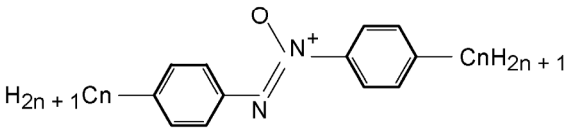

(a)

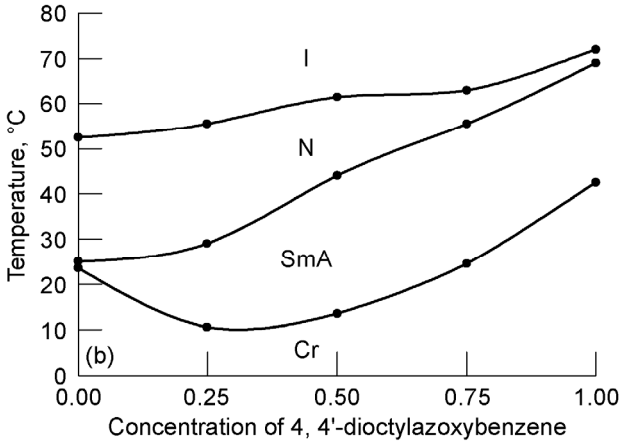

Figure 5.—Molecular structure of 4, 4'-n-dialkylazoxybenzene (a); Phase diagram of the binary mixture of n = 6 and n = 8 homologues of 4, 4'-n-dialkylazoxybenzene (b).

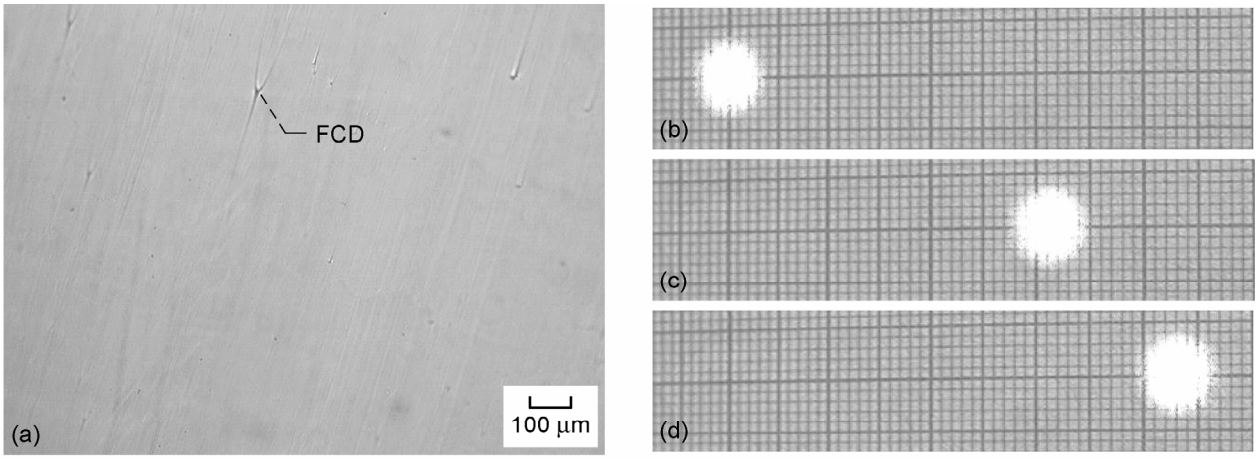

Figure 6.—(a) Textures observations of the wedge cell filled with the SmA mixture after alignment in 1.2 T magnetic field. Thickness of the cell ~200 μm, wedge angle ~9.2°. (b) Position of the incident beam on the screen. (c) Position of the deflected ordinary beam passed through the wedge cell. (d) Position of the deflected extraordinary beam.

3. Optical Elements: SmA-Filled Prisms and Lattices

3.1 Single SmA Prisms

The geometry of the prismatic cell filled with LC material is shown in figure 1. Two glass plates with rubbed polyimide layers (PI2555, Microsystems) formed a wedge cell, which was filled with the SmA blend of 4,4'-dihexylazoxybenzene and 4,4'-dioctylazoxybenzene in proportion 1:1. The assembled cell was heated to the isotropic state and slowly cooled down to room temperature with the temperature rate $\sim 5\times10^{-4}$ K/s in 1.2 T magnetic field. The measured parameters of the birefringent prism are as following:

- wedge angle: 9.2°;
- refractive indices of the SmA mixture (at λ = 633 nm and temperature 22 °C): $n_e = 1.72\pm0.01$, $n_o = 1.53\pm0.01$, $\Delta n = 0.19$;
- steering angles: for the light polarized parallel to the LC director (extraordinary wave) $\theta_e = 6.7°$, for the light polarized perpendicular to the LC director (ordinary wave) $\theta_o = 4.9°$.

The textures of the aligned mixture (fig. 6(a)) show a small amount of residual FCDs. As the SmA mixture has a positive birefringence $\Delta n = n_e - n_o > 0$, the extraordinary wave will deflect more than the ordinary wave (fig. 6(b) to (d)). In figure 7 we show the transmission of the extraordinary and ordinary waves through the wedge in SmA (t = 25 °C) and nematic phases (t = 48 °C) at wavelength λ = 633 nm. The photodetector was placed at the distance 22 cm from the sample. The diameter of the probing laser beam was about 2 mm. The data are normalized by the incident light intensity I_0. Figure 7 clearly demonstrates that the SmA phase is much more transparent than the nematic phase due to reduction of light scattering at the director fluctuations. The transmission of SmA phase remains above 70 percent for both ordinary and extraordinary components even when the LC layer becomes thicker than 1 mm. The variations of light transmission with thickness observed in the plots in figure 7 for SmA are caused by the residual amount of FCDs in different regions of the wedge shaped cell used for the measurements.

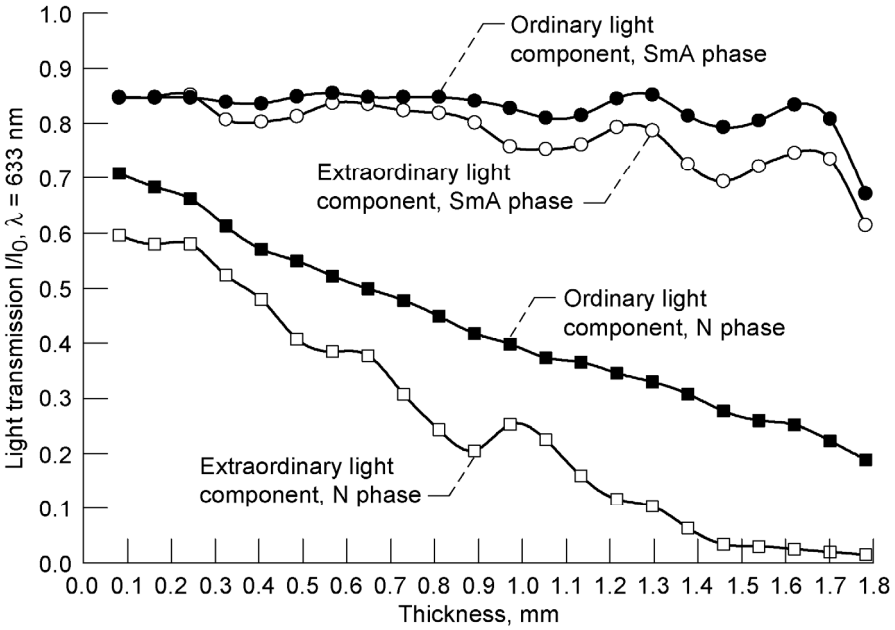

Figure 7.—Transmission of the birefringent wedge cell at λ = 633 nm.

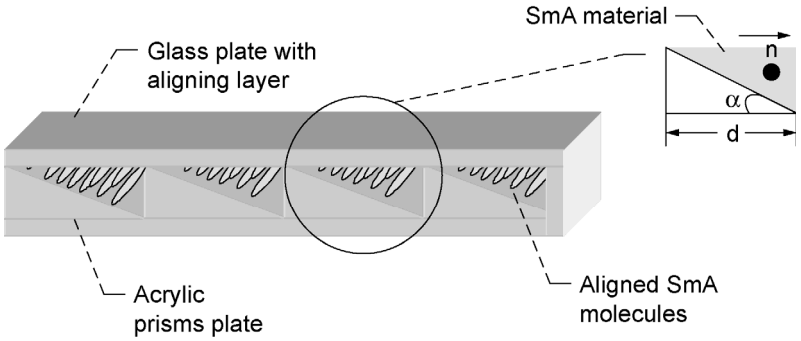

Figure 8.—Sketch of the array of polymer prisms filled with the SmA material.

3.2 Polymer Array of Prisms Filled With SmA Material

The assembling of the SmA-filled wedges for the wide-aperture incident beam requires large quantities of LC material. A more practical approach might be to replace a single birefringent prism with an array of smaller prisms, at the expense of some decrease in light transmission efficiency caused by light diffraction, destructive interference, and non-ideal profile. Hirabayashi et al. reported on quartz microprisms filled with the nematic material, which can deflect closely spaced micro-optical beams individually to any position with a high transmittance, high deflection angle and low voltage (ref. 39). Here we describe an array of prisms filled with a SmA material. Right angle prisms may be molded in a sheet of polymer material with a different cut angle *a* and period *d* (fig. 8). We used the array of prisms formed in an acrylic film of optical quality with the refractive index $n = 1.49$ (at $\lambda = 589$ nm) with $a = 30°$ and $d = 1$ mm (purchased from Fresnel Technologies, Inc.) The acrylic array of prisms was attached to a glass substrate coated with rubbed polyimide PI2555 to align the director along the grooves. Then the assembled cell was filled with the 1:1 (by weight) mixture of 4,4'-dihexylazoxybenzene and 4,4'-dioctylazoxybenzene. After magnetic field alignment, we measured the deflection efficiency and deflection angles of the cell at 633 nm for normal incidence at the room temperature (we considered the

zero-order diffracted beam; the diameter of the incident beam was 5 mm; the cell was illuminated from the glass plate side):

- for the extraordinary wave, the deflection efficiency was ~75.4 percent and the deflection angle $\theta_e = 7.2° \pm 0.2°$;
- for the ordinary wave, the deflection efficiency was ~80.5 percent and the deflection angle $\theta_o = 0.6° \pm 0.2°$.

The performance of the assembled cell is very similar to Rochon prisms, but due to a slight mismatch between the acrylic refractive index and ordinary refractive index of the LC material the ordinary wave is slightly deflected. We checked the temperature dependence of the deflection characteristics of SmA-filled microprisms. The temperature-induced changes in the deflection angles were relatively small, about 0.02° per 1 °C for the extraordinary and less than that for the ordinary wave. Thus, with the temperature increase from 15 to 40 °C the deflection angles changed from 7.14° to 6.68° for the extraordinary beam and from 0.61° to 0.56° for the ordinary beam.

The light propagation through the array of prisms is affected by the geometry of the prisms which is far from the ideal triangular profile. In figure 9 we show the fluorescent confocal microscopy (ref. 40) images of the prisms filled with the mixture of Cargille™ refractive index fluid ($n_d = 1.52$) and Nile Red (Aldrich) fluorescent dye (0.01% by weight). The prisms profile is not regular, which is the reason for a difference (of about 0.2°) between the measured and theoretically calculated values of the deflection angles.

4. Polarization Rotators

We used 90° TN cells as electrically-controlled polarization rotators. The cells were assembled from two glass plates with indium tin oxide (ITO) layers and covered by rubbed polyimide PI2555 (Microsystems), which provides planar orientation of the LC molecules. Easy axes of the nematic director are mutually orthogonal at the opposite substrates. The cells were filled with the mixture of dual-frequency nematic mixture MLC-2048 (Merck, optical birefringence $\Delta n = 0.22$ at $\lambda \approx 633$ *nm*) and right-handed chiral dopant R1011 (Merck, 0.05% by weight).

Depending on the applied voltage, the TN cell can be either in the “OFF or “ON” state. (fig. 1). In the OFF state, the cell rotates the polarization of the linearly polarized beam by 90°. The emerging light remains linearly polarized only if the TN cell satisfies one of two criteria: (1) either it is infinitely thick and satisfies the Mauguin limit ($\lambda << d\ \Delta n$) or (2) its thickness d satisfies the conditions of so-called Gooch-Tarry or Mauguin minima (ref. 41):

$$d = \frac{\lambda}{2\Delta n}\sqrt{4m^2 - 1};\ m = 1,2,3,... \tag{6}$$

In the ON state of the TN cell, the direction of light polarization remains the same. An applied voltage realigns the nematic director perpendicular to the plates and the optical activity disappears. We used the TN cells of thickness $d \approx 5.6$ μm to satisfy the condition of the second minimum (ref. 41) at $\lambda =$ 633 nm. We measured the optical transmission of the TN cells with antireflective coatings at $\lambda = 633$ nm. The transmission coefficient (the ratio of the output beam intensity to the incident beam intensity) was 94 percent for the OFF state and 97 percent for the ON state.

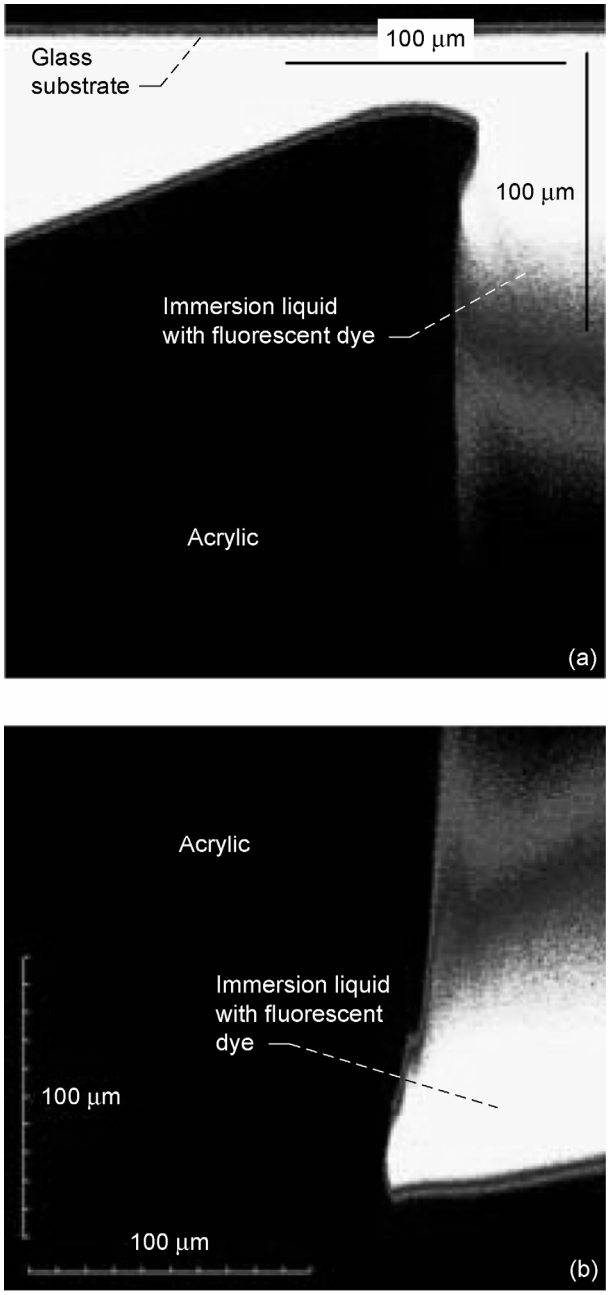

Figure 9.—Confocal microscopy study of the polymer prisms array. (a) Apex of one acrylic prism of the array. (b) Base of the acrylic prism.

Figure 10 shows the typical time dependence of the transmission of the TN cell placed between crossed polarizers at $\lambda = 633$ nm. The optical signal shows good stability for both ON and OFF states of the TN cell under application of the repetitive driving voltage (fig. 10(a)). To avoid a back flow effect (nematic material flows caused by director reorientation) we applied holding and kick-off voltage pulses with properly adjusted amplitudes. For example, we used $U_{rms,\ hold,\ 1kHz} = 6$ V and $U_{rms,\ hold,\ 50kHz} = 4$ V to hold 5.6 μm thick TN cell in the homeotropic and in the twisted state, respectively. In order to minimize a dielectric heating effect we applied high-amplitude pulses for a short time, 0.5 and 0.25 ms, at frequencies

2 and 50 kHz, respectively. With these pulses we were driving the TN cell continuously for hours but did not observe a worsening of the transmission signal caused by the dielectric heating effect.

By applying the driving voltage with high-amplitude kick-off voltage pulses, we achieved the switching time of about 0.5 ms for ON (fig. 10(b)) and about 0.25 ms for OFF (fig. 10(c)) states. The kick-off voltage pulses are applied either at low (f = 2 kHz) or high (f = 50 kHz) frequencies, to switch the dual-frequency nematic material into ON or OFF states, respectively (the dielectric anisotropy of MLC-2048 is positive below some critical frequency f_c and negative at $f > f_c$, where $f_c \approx 12$ kHz for MLC-2048 mixture at the temperature 20 °C). The application of an amplitude and frequency modulated waveform for driving of a dual-frequency nematic has an obvious advantage in comparison with a conventional nematic driving scheme where the high-frequency pulses are absent. For example, we achieved a response time of about 30 ms with the same cell when no high-frequency signal is applied and the cell is relaxing from the ON to OFF state due to restoring elastic forces. A much faster switching of 0.25 ms is achieved with application of high-frequency voltage pulses (fig. 10(c)).

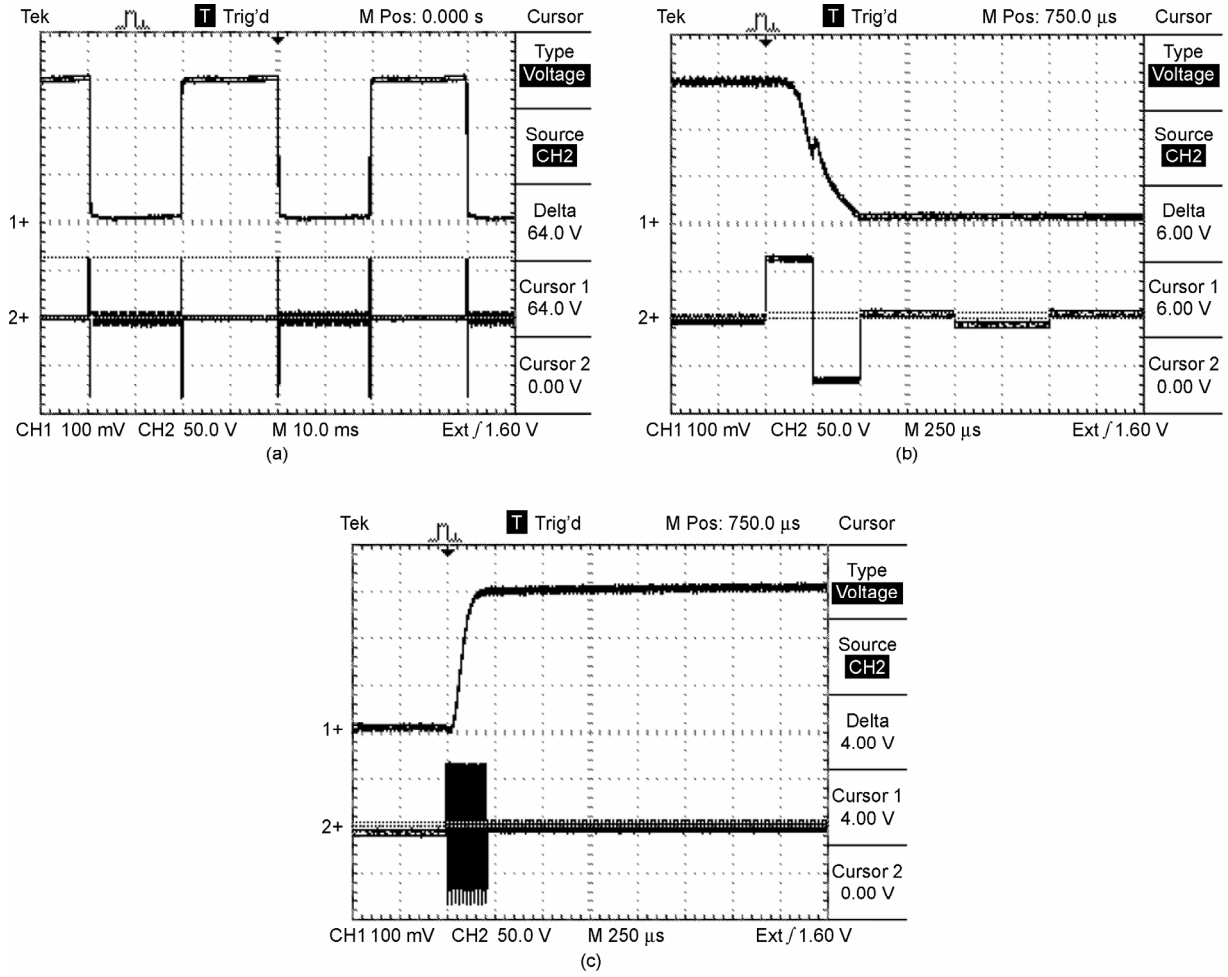

Figure 10.—Oscilloscope pictures demonstrating the optical transmittance of the 90° TN cell (top traces) filled with dual-frequency nematic material (crossed polarizers, cell thickness 5.6 µm) versus the applied voltage (bottom traces). (a) Fast linear polarization switching with repetition rate of 25 Hz. Time scale 10 ms/sqr. (b) Transition of TN cell to the homeotropic state by application of the low-frequency kick-off voltage pulses (64 V RMS, f = 2 kHz), followed by the low-frequency holding voltage (6 V RMS, f = 1 kHz). Time scale 250 µs/sqr. (c) Transition of TN cell to the planar state by application of high-frequency kick-off voltage pulses (64 V RMS, f = 50 kHz), followed by the high-frequency holding voltage (4 V RMS, f = 50 kHz). Time scale 250 µs/sqr .

5. Conclusions

We demonstrated the applicability of SmA materials in birefringent prisms and arrays. SmA elements can be used in non-mechanical DBDs that are based on decoupled pairs of electrically-controlled liquid crystalline polarization rotators, such as TN cells and passive deflectors. This approach allows one to separate the issue of time response and beam deflection angles and optimize these two parameters separately. We achieved fast (0.5 msec) response time of dual-frequency nematic 90° TN cells by implementing a dual-frequency nematic and overdriving scheme of electrical switching, where an electrical signal is a sequence of high-amplitude pulses (64 V rms, at 2 and 50 kHz) and holding voltages (6 and 4 V rms at 1 and 50 kHz, respectively).

The deflection angles can be optimized by the design of the birefringent prisms. SmA-filled prisms are attractive in low-cost applications where one needs large apertures, large angles of deflection, and/or non-trivial geometries. We demonstrated that mixtures of homologues of 4,4'-*n*-dialkylazoxybenzene produce SmA phases with a broad temperature range of SmA existence (up to 30 °C for binary mixtures) with a relatively small number of residual defects, such as focal conic domains, and high transmission characteristics. We determined the typical magnetic fields needed to remove director distortions around the mechanical inclusions and focal conic domains. Magnetic alignment is most effective when the material is aligned in the nematic phase and then cooled down to the SmA phase.

The SmA-filled birefringent prisms have certain advantages as compared to the crystalline prisms. The SmA prisms are easier and cheaper to form. The optical axis of SmA prisms can be controlled by surface alignment. They can be prepared as relatively thick prisms (up to 7 mm in our case) or as arrays of (micro) prisms. Light scattering in SmA birefringent prisms can be reduced by proper alignment to levels that are significantly lower than light scattering at the director fluctuations in the nematic samples of the same thickness. As the light scattering is caused mostly by FCDs that have a fixed size, it becomes smaller with the increase of the wavelength of light; the IR part of the spectrum is less sensitive to these losses. Thus, the SmA prisms are suitable candidates for beam steering not only in the visible part of the spectrum, but in the infrared part as well. An obvious drawback of the SmA prisms is that they can be used only within the temperature range of the SmA phase. The latter can be expanded significantly by using mixtures, as in this work.

References

1. P.F. McManamon, E.A. Watson, T.A. Dorschner, and L.J. Barnes, "Applications Look at the Use of Liquid-Crystal Writable Gratings for Steering Passive Radiation," *Opt. Eng.* 32(11), 2657–2664 (1993).
2. J.A. Thomas and Y. Fainman, "Optimal Cascade Operation of Optical Phased-Array Beam Deflectors," *Appl. Opt.* 37(26), 6196–6212 (1998).
3. O. Solgaard, F.S.A. Sandejas, and D.M. Bloom, "Deformable Grating Optical Modulator," *Opt. Lett.* 17(9), 688–690 (1992).
4. R. Fuchs, H. Jerominek, N. Swart, Y. Diawara, M. Lehoux, G. Bilodeau, S. Savard, F. Cayer, Y. Rouleau, and P. Lemire, "Novel Beam Steering Micromirror Device," *Proc. SPIE* 3513, 40–49 (1998).
5. J.-H. Kim, L. Sun, C.-H. Jang, C.-C. Choi, and R.T. Chen, "Polymer-Based Thermo-Optic Waveguide Beam Deflector with Novel Dual Folded-Thin-Strip Heating Electrodes," *Opt. Eng*. 42(3), 620–624 (2003).
6. D. Kang, J.E. Maclennan, N.A. Clark, A. Zakhidov, and R.H. Baughman, "Electro-Optic Behavior of Liquid-Crystal-Filled Silica Opal Photonic Crystals: Effect of Liquid-Crystal Alignment," *Phys. Rev. Lett.* 86(18), 4052–4055 (2001).
7. W. Klaus, "Development of LC Optics for Free-Space Laser Communications," *AEU-International Journal of Electronics and Communications* 56(4), 243–253 (2002).

8. S.-T. Wu, M.E. Neubert, S.S. Keast, D.G. Abdallah, S.N. Lee, M.E. Walsh, and T.A. Dorschner, "Wide Nematic Range Alkenyl Diphenyldiacetylene Liquid Crystals," *Appl. Phys. Lett.* 77(7), 957–959 (2000).
9. A.B. Golovin, S.V. Shiyanovskii, and O.D. Lavrentovich, "Fast-Switching Dual-Frequency Liquid Crystal Optical Retarder, Driven by an Amplitude and Frequency Modulated Voltage," *Appl. Phys. Lett*. 83(19), 3864–3866 (2003).
10. J. Borel, J.C. Deutsch, G. Labrunie, and J. Robert, "Liquid Crystal Diffraction Grating," US Patent 3,843,231 (22 October 1974).
11. G. Williams, N.J. Powell, A. Purvis, and M.G. Clark, "Electrically Controlled Liquid Crystal Fresnel Lens," *Proc. SPIE* 1168, 352–357 (1989).
12. B.J. Cassarly, J.C. Ehlert, and D.J. Henry, "Low Insertion Loss High Precision Liquid Crystal Optical Phased Array," *Proc. SPIE* 1417, 110–121 (1991).
13. X. Wang, D. Wilson, R. Muller, P. Maker, and D. Psaltis, "Liquid-Crystal Blazed-Grating Beam Deflector," *Appl. Opt*. 39(35), 6545–6555 (2000).
14. C.M. Titus, J.R. Kelly, E.C. Gartland, S.V. Shiyanovskii, J.A. Anderson, and P.J. Bos, "Asymmetric Transmissive Behavior of Liquid-Crystal Diffraction Gratings," *Opt. Lett.* 26(15), 1188–1190 (2001).
15. R.L. Sutherland, V.P. Tondiglia, L.V. Natarajan, T.J. Bunning, and W.W. Adams, "Electrically Switchable Volume Holographic Gratings in Polymer-Dispersed Liquid Crystals," *Appl. Phys. Lett*. 64(9), 1074–1076 (1994).
16. P. Berthele, E. Gros, B. Fracasso, J.L.D. De la Tochnaye, "Efficient Beam Steering in the 1.55 Micron Window Using Large-Tilt FLC One Dimensional Array," *Ferroelectrics* 214(1–2), 791–798 (1998).
17. D. Subacius, S.V. Shiyanovskii, P. Bos, and O.D. Lavrentovich, "Cholesteric Gratings with Field-Controlled Period," *Appl. Phys. Lett.* 71(23), 3323–3325 (1997).
18. A.Y.-G. Fuh, C.-H. Lin, and C.-Y. Huang, "Dynamic Pattern Formation and Beam Steering Characteristics of Cholesteric Gratings," *Jpn. J. Appl. Phys*. 41(1), 211–218 (2002).
19. U.J. Schmidt,"A High Speed Digital Light Beam Deflector," *Phys. Let*., 12(3), 205–206 (1964).
20. W. Kulchke, K. Kosanke, E. Max, M.A. Haberger, T.J. Harris, and H. Fleisher, "Digital Light Deflectors," *Appl. Opt.* 5(10), 1657–67 (1966).
21. H. Meyer, D. Riekmann, K.P. Schmidt, U.J. Schmidt, M. Rahlff, E. Schroder, and W. Thust, "Design and Performance of a 20-Stage Digital Light Beam Deflector," *Appl. Opt*. 11(8), 1732–1736 (1972).
22. C.M. Titus, P.J. Bos, and O.D. Lavrentovich, "Efficient Accurate Liquid Crystal Digital Light Deflector," *Proc. SPIE* 3633, 244–253 (1999).
23. C.M. Titus, "Refractive and Diffractive Liquid Crystal Beam Steering Devices," *Dissertation, Chemical Physics Interdisciplinary Program, Kent State University*, pp. 34–36 (2000).
24. D.-F. Gu, B. Winker, D. Taber, J. Cheung, Y. Lu, P. Kobrin, and Z. Zhuang, "Dual Frequency Liquid Crystal Devices for Infrared Electro-Optical Applications," *Proc. SPIE*, 4799, 37 (2002).
25. S.A. Khan and N.A. Riza, "Demonstration of Three-Dimensional Wide Angle Laser Beam Scanner Using Liquid Crystals," *Opt. Express*, 12(5), 868–882 (2004).
26. O. Pishnyak, L. Kreminska, O.D. Lavrentovich, J.J. Pouch, F.A. Miranda, and B.K. Winker, "Digital Beam Steering Device Based on Decoupled Birefringent Prism Deflector and Polarization Rotator," NASA/TM—2004-213197.
27. L.M. Blinov and V.G. Chigrinov, *Electrooptic Effects in Liquid Crystal Materials*, Springer-Verlag, New York, Inc. (1994).
28. P.G. de Gennes and J. Prost, *The Physics of Liquid Crystals*, 2nd ed., Clarendon Press, Oxford (1993).
29. G. Vertogen and W.H. de Jeu, *Thermotropic Liquid Crystals, Fundamentals*, Springer-Verlag, Berlin (1988).
30. M. Kleman and O.D. Lavrentovich, *Soft Matter Physics: An Introduction*, Springer, NY (2003).
31. G.R. Luckhurst, "Field-Induced Alignment of the Directors in the Smectic A Phase. Experiment and Simulation," *Mol. Cryst. Liq. Cryst.* 347(part II), 121–135 (2000).

32. G.R. Luckhurst, T. Miyamoto, A. Sugimura, and B.A. Timimi, "Electric Field-Induced Alignment of the Directors in the Smectic A Phase of 4-Octyl-4'-Cyanobiphenyl. A Deuterium NMR Study," *Mol. Cryst. Liq. Cryst.* 347(part II), 147–156 (2000).
33. Y. Takanishi, Y. Ouichi, H. Takezoe, and A. Fukuda, "Chevron Layer Structure in Smectic A Phase of 8CB," *Jpn. J. Appl. Phys. Lett.* 28(3), L487–489 (1989).
34. O. Ou Ramdane, P.h. Auroy, S. Forget, E. Raspaud, P.h. Martinot-Lagarde, and I. Dozov, "Memory-Free Conic Anchoring of Liquid Crystals on a Solid Substrate," *Phys. Rev. Lett.* 84(17), 3871–3874 (1994).
35. O.D. Lavrentovich, M. Kleman, and V.M. Pergamenshchik, "Nucleation of Focal Conic Domains in Smectic A Liquid Crystals," *J. Phys. II* 4(2), 377–404 (1994).
36. O.D. Lavrentovich and M. Kleman, "Field-Driven First-Order Structural Transition in the Restricted Geometry of a Smectic A Cell," *Phys. Rev. E* 48(1), R39-R42 (1993).
37. M. Kleman and O.D. Lavrentovich, "Curvature Energy of a Focal Conic Domain with Arbitrary Eccentricity," *Phys. Rev. E* 61(2), 1574–1578 (2000).
38. Z. Li and O.D. Lavrentovich, "Surface Anchoring and Growth Pattern of the Field-Driven First-Order Transition in a Smectic-A Liquid Crystal," *Phys. Rev. Lett.* 73(2), 280–283 (1994).
39. K. Hirabayashi, T. Yamamoto, and M. Yamaguchi, "Free-Space Optical Interconnections with Liquid-Crystal Microprism Arrays," *Appl. Opt.* 34(14), 2571–2580 (1995).
40. I.I. Smalyukh, S.V. Shiyanovskii, and O.D. Lavrentovich, "Three-Dimensional Iimaging of Orientational Order by Fluorescence Confocal Polarizing Microscopy," *Chem. Phys. Lett.* 336, 88–96, (2001).
41. C.H. Gooch and H.A. Tarry, "The Optical Properties of Twisted Nematic Liquid Crystal Structures with Twist Angles ≤90°," *J. Phys. D.: Appl. Phys*. 8(13), 1575–84 (1975); C.H. Gooch and H.A. Tarry, "Optical Characteristics of Twisted Nematic Liquid-Crystal Films," *Electron. Lett*. 10(1), 2–4 (1974).

REPORT DOCUMENTATION PAGE

Form Approved
OMB No. 0704-0188

1. AGENCY USE ONLY (*Leave blank*)	2. REPORT DATE	3. REPORT TYPE AND DATES COVERED
	September 2006	Technical Memorandum

4. TITLE AND SUBTITLE

Smectic A Filled Birefringent Elements and Fast Switching Twisted Dual Frequency Nematic Cells Used for Digital Light Deflection

5. FUNDING NUMBERS

WBS–22–612–30–81–04

6. AUTHOR(S)

Oleg Pishnyak, Andrii Golovin, Liubov Kreminska, John J. Pouch, Félix A. Miranda, Bruce K. Winker, and Oleg D. Lavrentovich

7. PERFORMING ORGANIZATION NAME(S) AND ADDRESS(ES)

National Aeronautics and Space Administration
John H. Glenn Research Center at Lewis Field
Cleveland, Ohio 44135–3191

8. PERFORMING ORGANIZATION REPORT NUMBER

E–15406

9. SPONSORING/MONITORING AGENCY NAME(S) AND ADDRESS(ES)

National Aeronautics and Space Administration
Washington, DC 20546–0001

10. SPONSORING/MONITORING AGENCY REPORT NUMBER

NASA TM—2006-214049

11. SUPPLEMENTARY NOTES

Prepared for publishing in Optical Engineering, SPIE, Bellingham, Washington. Oleg Pishnyak, Andrii Golovin, Oleg D. Lavrentovich, and Liubov Kreminska, Kent State University, Liquid Crystal Institute, P.O. Box 5190, Kent, Ohio 44242; John J. Pouch and Félix A. Miranda, NASA Glenn Research Center; Bruce K. Winker, Rockwell Scientific Company LLC, 1049 Camino Dos Rios, Thousand Oaks, California 91360. Responsible person, John J. Pouch, organization code RCA, 216–433–3523.

12a. DISTRIBUTION/AVAILABILITY STATEMENT

Unclassified - Unlimited
Subject Category: 74

Available electronically at http://gltrs.grc.nasa.gov

This publication is available from the NASA Center for AeroSpace Information, 301–621–0390.

12b. DISTRIBUTION CODE

13. ABSTRACT ***(Maximum 200 words)***

We describe the application of smectic A (SmA) liquid crystals for beam deflection. SmA materials can be used in digital beam deflectors (DBDs) as fillers for passive birefringent prisms. SmA prisms have high birefringence and can be constructed in a variety of shapes, including single prisms and prismatic blazed gratings of different angles and profiles. We address the challenges of uniform alignment of SmA, such as elimination of focal conic domains. Fast rotation of the incident light polarization in DBDs is achieved by an electrically switched 90° twisted nematic (TN) cell.

14. SUBJECT TERMS

Liquid crystal; Beam deflector; Birefringent prism; Smectic A; Polarization rotator

15. NUMBER OF PAGES

20

16. PRICE CODE

17. SECURITY CLASSIFICATION OF REPORT	18. SECURITY CLASSIFICATION OF THIS PAGE	19. SECURITY CLASSIFICATION OF ABSTRACT	20. LIMITATION OF ABSTRACT
Unclassified	Unclassified	Unclassified	